



Contents lists available at ScienceDirect

Inorganica Chimica Acta

journal homepage: www.elsevier.com/locate/ica

Coordination chemistry to palladium(II) of pyridylbenzamidine ligands and the related reactivity with ethylene

Andrea Tognon^a, Vera Rosar^a, Nicola Demitri^b, Tiziano Montini^a, Fulvia Felluga^a, Barbara Milani^{a,*}

^a Department of Chemical and Pharmaceutical Sciences, University of Trieste, Via Licio Giorgieri, 1, 34127 Trieste, Italy

^b Elettra – Sincrotrone Trieste, S.S. 14 Km163.5 in Area Science Park, 34149 Basovizza, Trieste, Italy

ARTICLE INFO

Article history:

Received 4 November 2014

Received in revised form 21 January 2015

Accepted 25 January 2015

Available online xxx

Keywords:

Pyridylbenzamidine

Palladium

Coordination chemistry

Ethylene

ABSTRACT

The coordination chemistry to palladium of three pyridylbenzamidines (N-N') was investigated in detail. The studied pyridylbenzamidines are featured by the bulky 2,6-diisopropylphenyl substituent at the azomethine nitrogen atom of the amidine unit, and differ in the substitution either at the amino atom, which bears a 2-pyridyl or a 6-methyl-2-pyridyl group, or at the bridging N-atom that, in one case, is substituted by a methyl group, leading to a molecule reported herein for the first time. The accurate NMR characterization of the free ligands points out the presence of dynamic phenomena in solution, due to the interconversion of several possible isomers, including tautomers. The coordination chemistry to Pd(II) is studied using both [Pd(cod)(CH₃)Cl] and [Pd(cod)(CH₃)(CH₃CN)][PF₆]₂ as metal precursor. Depending on the palladium precursor and on the pyridylbenzamidine, different coordination compounds are obtained, demonstrating the capability of these molecules to act both as mono- and bidentate ligands. For the pyridylbenzamidine substituted with the methyl group on the bridging N-atom, the C–H activation of one of the isopropyl groups is observed with the formation of a six-membered palladacycle and methane. None of the isolated complexes generates active catalysts either for ethylene homopolymerization or for ethylene/methyl acrylate copolymerization. When reacting with ethylene, the complexes lead to the formation of propylene and the inactive dicationic [Pd(N-N')₂][PF₆]₂ complex.

© 2015 Elsevier B.V. All rights reserved.

1. Introduction

Starting from Brookhart's discovery that Ni(II) and Pd(II) complexes with α -diimine ligands are extremely efficient catalysts for alkene polymerization [1], the last two decades have witnessed a huge development of complexes based on late transition metals and nitrogen-donor ligands for application as catalysts in polyolefin synthesis [2,3].

This discovery opened the possibility for using late transition metal complexes as catalysts for the ethylene/polar vinyl monomer copolymerization to yield functionalized polyolefins, a highly challenging reaction [4–12]. In particular, focusing the discussion on nitrogen-donor ligands, the catalytic systems reported in the literature are based on palladium(II) complexes with α -diimines having an acenaphthene (BIAN) or a 1,4-diaza-1,3-butadiene (DAB) skeleton and, on the iminic nitrogen atoms, aryl rings substituted in *ortho* position with bulky groups [13,14]. These led to the formation of amorphous, branched ethylene/methyl acrylate (MA) copolymers with an activity of 57 g CP/g Pd-h (g CP/g Pd-h = grams

of copolymer per gram of palladium per hour), a content of inserted polar monomer in the range 4–25% depending on the substituent on the aryl rings and with the polar monomer inserted at the end of the branches [13,14]. A palladium complex with a cyclophane-modified BIAN was reported to catalyze the same reaction with an activity of 1.6 g CP/g Pd-h and a content of incorporated MA up to 21.8% [15]. α -diimines with different skeletons were also studied leading, however, to poorly active catalysts [16]. The content of incorporated acrylate was increased up to 37% by using Pd(II) complexes with α -diimines substituted by 1-naphthyl groups [17].

All the studied α -diimines are characterized by the same aryl rings on the donor atoms. Recently, we introduced a new nonsymmetrically substituted α -diimine having one aryl ring *meta*-substituted with an electron-withdrawing group and the other ring *ortho*-substituted with an electron-releasing group (Fig. 1) [18]. The corresponding Pd(II) complex was found to be twice as productive as the catalyst with the symmetrically *ortho*-substituted ligand and leading to the ethylene/MA co-oligomer with a higher content of incorporated polar monomer, thus pointing out the positive effect of the subtle unbalance of the electronic and steric properties of the nitrogen-donor atoms. The same effect was previously observed by some of us in the CO/vinyl arene

* Corresponding author. Tel.: +39 040 5583956.

E-mail address: milaniba@units.it (B. Milani).

copolymerization catalyzed by Pd(II) complexes with nonsymmetrically *meta*-substituted BIANs [19,20].

With the aim to illustrate the beneficial effect of nonsymmetric ancillary ligands, we have now investigated the coordination chemistry to palladium, and the catalytic behavior of related complexes in the ethylene/MA copolymerization, of bidentate nitrogen-donor ligands belonging to the family of pyridylbenzamidines molecules (Scheme 1). These ligands are characterized by one pyridinic and one iminic nitrogen atom plus an additional nitrogen on the bridge connecting the two moieties of the ligand. Upon coordination to palladium a six-membered palladacycle should result with structural features, like the N–Pd–N bond angle close to the values of ideal square planar complexes, that might have positive effects in catalysis. Indeed, when studying the CO/styrene copolymerization we found that moving from bis(oxazolines) (5-membered Pd-cycle) to azabis(oxazolines) (6-membered Pd-cycle, with a nitrogen atom bridging the two oxazoline rings) a remarkable increase in the catalytic performance of the related Pd(II) complexes was achieved together with an increase in catalyst stability [21].

Ligands **1** and **2** (Scheme 1) were previously reported as having been applied to prepare both palladium(II) and nickel(II) complexes, which were tested as precatalysts for the Suzuki–Miyaura reaction and ethylene oligomerization, respectively [22,23]. Pd(II) and Ni(II) complexes with bis(pyridyl)-N-alkylaminato ligands were reported to be active catalysts for ethylene dimerization to a mixture of 1- and 2-butenes [24,25]. Ligand **3** is reported herein for the first time.

2. Results and discussion

2.1. Synthesis and characterization of ligands 1–3

N-pyridylbenzamidines **1–3** share the presence of the bulky 2,6-diisopropylphenyl (2,6-diisopropylphenyl = dip) substituent at the azomethine (N_{imino}) nitrogen atom of the amidine unit. Compounds **1** and **2** differ in the nature of the substitution at the amino (N_{amino}) atom, which bears a 2-pyridyl and a 6-methyl-2-pyridyl group, respectively; in compound **3** the acidic N-hydrogen atom is replaced by a N-methyl group (Scheme 1).

The synthesis reported in the literature of **1** [23] and **2** [22] follows a classical route for the preparation of N,N'-disubstituted amidines [26,27]. It proceeds through the reaction of the imidoylchloride with 2-aminopyridine or 6-methyl-2-aminopyridine respectively, affording **1** and **2** in approximately 50% yield (Scheme 1). This approach was extended to the synthesis of **3**, by using N-methylaminopyridine as the amine partner [28]. However, the reaction required modification and optimization, as the secondary amine failed to react with the imidoylchloride under the above conditions, probably due to steric reasons. The lack of reactivity was circumvented by deprotonating the secondary amino group *in situ* with NaH, added in excess to the reaction mixture, leading to **3** in a 30% overall yield after purification (Scheme 1).

An alternative approach, involving deprotonation of the central N_{amino} nitrogen atom of **1** with NaH and subsequent trapping of the anion with CH₃I led to complex mixtures of unidentified

products. This method had previously proved to be successful in the base mediated N-alkylation of the bridging nitrogen atom of 2,2'-dipyridylamine ligands [24] and of aza-bis(oxazoline) compounds [29].

The structural characterization of **1–3** is not trivial as a number of different isomeric forms are possible for these compounds. Considering only the *E* geometry of the C=N double bond, as the *Z* is known to be disfavored in N,N'-disubstituted benzamidines [30], tautomers stem from the presence of the secondary amino group, while *s-cis* and *s-trans* conformations are the result of rotational isomerism with respect to the C–N_{amino} single bond, having a partial double bond character. In addition, hindered rotation around N-dip and the different relative position of the pyridinic N and the C=N bond must be taken into account (Scheme 2). Complex equilibria between isomers and tautomers in solution have been already described for bulky non symmetric N,N'-diarylbenzamidines [31–33]. Useful information about the structure of pyridylbenzamidines **1–3** comes from the X-ray crystallographic structure of N-dip-N'-5-(nitropyridyl)benzamidines [23], and of N-phenyl-N'-pyridylbenzamidines [34], which showed that these compounds crystallized in the expected *E* configuration of the C=N double bond, with an *anti* relative position of the N_{pyridino} and N_{imino} atoms, and an *s-cis* conformation around the C–N_{amino} bond, as represented in Scheme 2.

Ligands **1** and **2** were isolated as light yellow solids, and characterized by ESI-MS, and NMR spectroscopy. The ¹H NMR spectra (CD₂Cl₂, r.t.) showed in the range of aliphatic protons two signals for the isopropyl methyl groups, at around 0.9 and 1.1 ppm, and two multiplets for the isopropyl CH protons at 3.0 and 3.3 ppm. These data are in agreement with those reported in the literature [23,22], where the different resonances were generically attributed to isomeric *E,syn* and *E,anti* mixtures. However, a deeper insight into the mono- and bidimensional spectra of **1** and **2** showed that the isopropyl methyl group signal at around 1.1–1.2 ppm was given, in both cases, by two overlapped doublets and that the area of the multiplets due to isopropyl CH protons did not correspond to one proton each, even though the relative total area matched for the expected number of protons (Figs. S3 and S5). In the COSY spectra the higher frequency CH signal (3.3 ppm) correlated with both CH₃ doublets, while the lower frequency CH (3.0 ppm) correlated only with the higher frequency CH₃ doublet (Figs. S4 and S6). NOESY analysis of **2** showed exchange peaks for both the CH and the methyl signals (Fig. S7).

Finally, in the aromatic range, together with the well resolved and intense peaks, large signals were also observed.

Although it was not obvious from these spectroscopic evidence which isomers were present, we assigned to **1** and **2** the exclusive *E,anti* configuration, and a preferential *s-cis* conformation around the C–N_{amino} single bond, with the large signals in the aromatic range and the multiple resonances for the methyl and CH hydrogen of the isopropyl groups being caused by dynamic phenomena in solution, such as hindered rotation around the C_{ipso}–N_{imino} bond and a slow equilibrium between tautomers.

The expected *anti* position of the N_{pyridino} and N_{imino} atoms was substantiated by the H³-pyridine chemical shift value (7.26 ppm) in **1** [35]; while the preference for the *s-cis* conformation was not

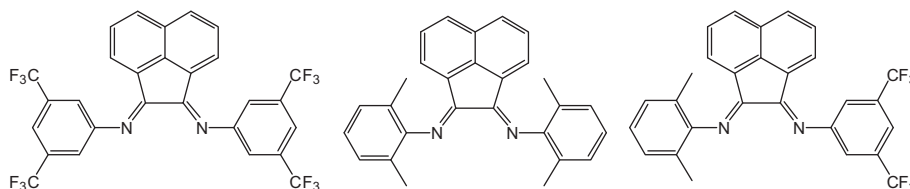
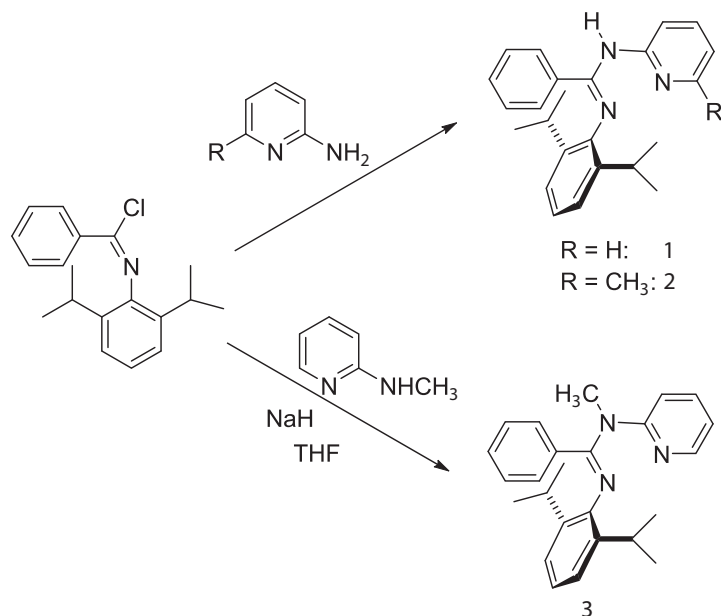
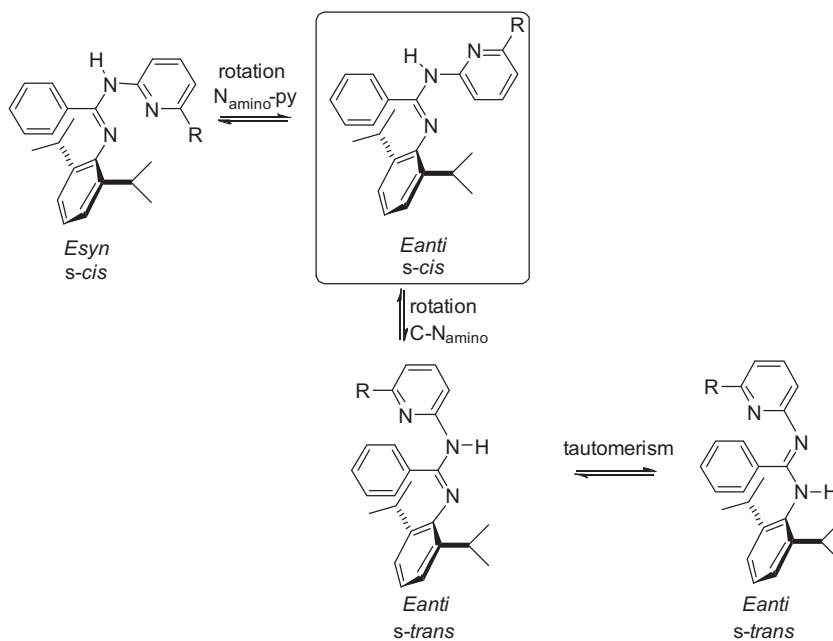


Fig. 1. The symmetric and nonsymmetric α -diimines studied [18].



Scheme 1. Synthetic scheme for ligands **1–3**.



Scheme 2. The equilibria among some of the possible isomeric forms in solution for *E* isomer of **1** and **2**.

only suggested by the above mentioned crystallographic structures, but also supported by data concerning *N,N'*-diphenylbenzamidine [30].

All these considerations were further confirmed by the observed simplification in the ^1H NMR spectrum of ligand **3**, where the tautomeric equilibrium is not possible. In fact only a single multiplet for the CH proton at 3.00 ppm was observed, which correlated with both methyl doublets, at 0.95 and 1.12 ppm, originated by the *N*-dip hindered rotation.

In the ^1H NMR spectrum of **3**, at room temperature, large signals were observed, in particular for *N*-CH₃ and for most of the aromatic and heteroaromatic protons. By lowering the temperature, up to 263 K, the resonances became sharp allowing their assignment (Fig. S8). Significantly, the H^3 -pyridine chemical shift, identified

at 6.65 ppm by correlation experiments, was lower than the one observed in **1** and **2**, suggesting a *syn* position of the pyridine nitrogen with respect to the $\text{C}=\text{N}_{\text{imino}}$, already shown to be the favorite also in *N*-methyl-*N*-phenyl-*N'*-(*p*-tolyl)benzamidine [30].

2.2. Coordination chemistry of ligands **1–3** to Pd(II)

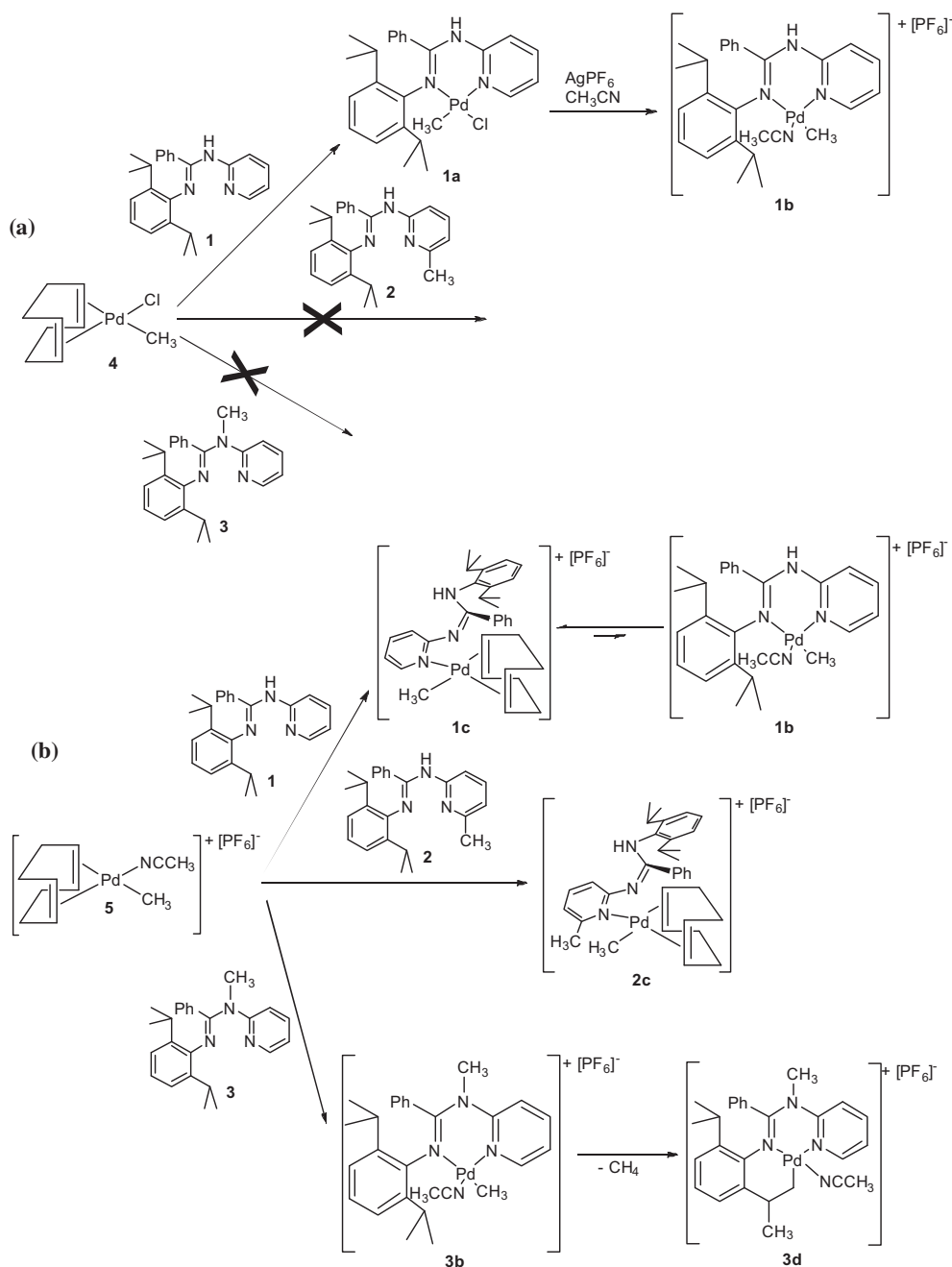
The coordination chemistry to Pd(II) of ligands **1–3** was studied by using two palladium precursors, $[\text{Pd}(\text{cod})(\text{CH}_3)\text{Cl}]$, **4**, and $[\text{Pd}(\text{-cod})(\text{CH}_3)(\text{CH}_3\text{CN})][\text{PF}_6]$, **5**. The synthesis of the latter is reported herein for the first time and it is based on the methodology applied to obtain the precursor $[\text{Pd}(\text{cod})(\text{CH}_3)(\text{OTf})]$ (OTf = triflate) [36], consisting in the abstraction of the halide from $[\text{Pd}(\text{cod})(\text{CH}_3)\text{Cl}]$, through the action of silver hexafluorophosphate in the presence

of acetonitrile. The NMR characterization in solution of complex **5**, obtained as a gray solid, was in agreement with its proposed structure (Figs. S11 and S12).

When ligand **1** was reacted with complex **4** under the usual reaction conditions [37,38,18], the coordination compound [Pd(**1**)(CH₃)Cl], **1a**, was obtained as a yellow solid (Scheme 3a), which was characterized by solution NMR spectroscopy using CD₂-Cl₂ as solvent, at room temperature. In the ¹H NMR spectrum, the number of signals and their integration indicated the presence in solution of one species (Fig. 2). No signal due to the free ligand was observed.

The main features of the ¹H NMR spectrum of **1a** were: the resonance of H⁶ remarkably shifted to a higher frequency with respect to the same signal in the spectrum of free ligand, indicating that the pyridyl ring is *cis* to the coordinated chloride ligand [39]; the

low frequency of the H³ doublet, compared to the same signal in the free ligand, confirming the *E,anti* conformation of **1** [35]; the 5.74 ppm shift to lower frequency of the broad signal of the bridging N–H due to the coordination; the presence of one multiplet and two doublets for the CH and the CH₃ groups of the isopropyl substituents, respectively, indicating the hindered rotation of the relevant aryl ring around the N–dip bond. This also confirmed that the two multiplets for the CH observed in the spectrum of **1** were caused by tautomerism, which is no longer possible after coordination to palladium; the singlet at 0.14 ppm due to the Pd–CH₃ fragment. The lower chemical shift of the latter group with respect to its typical value in analogous Pd–methyl complexes with nonsymmetric N-donor ligands [40,19,20] suggested that the methyl group experienced the shielding cone of the substituted aryl ring *cis* to it [41]. Indeed, NOE experiment performed upon



Scheme 3. Coordination chemistry of **1**, **2** and **3** to: (a) [Pd(cod)(CH₃)Cl]; (b) [Pd(CH₃)(CH₃CN)(cod)]PF₆.

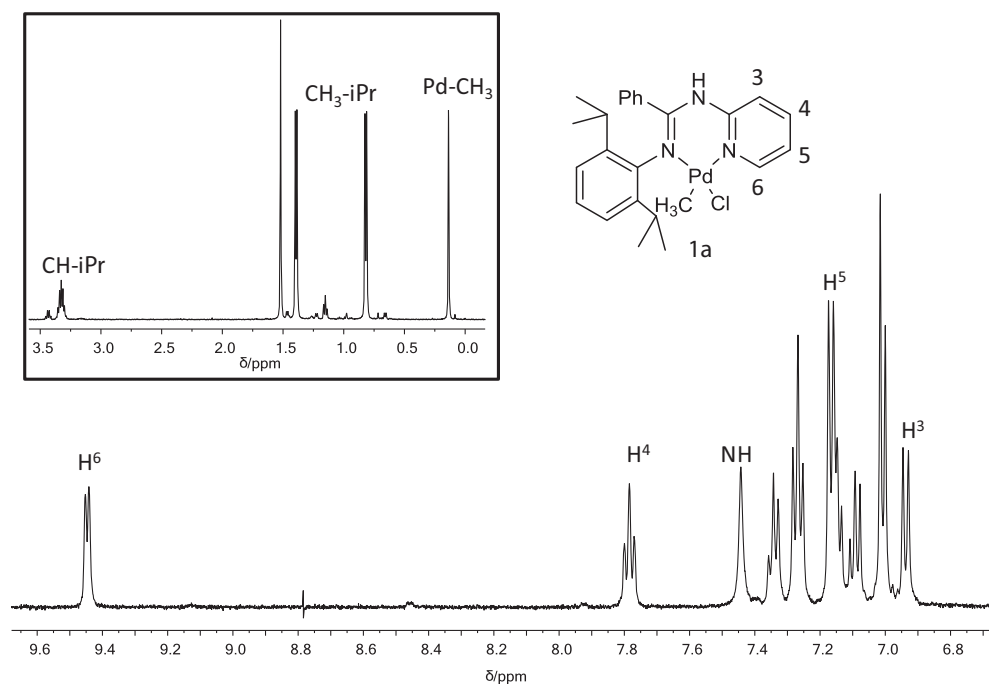


Fig. 2. ^1H NMR spectrum of **1a**, in CD_2Cl_2 , at 298 K, with the numbering scheme of the ligand. In the square the region of the aliphatic signals.

irradiation of this singlet demonstrated that this group was *cis* to dip (Fig. S15), confirming the presence of a single species of the two possible isomers differing in the relative position of the Pd- CH_3 fragment with respect to the two unequivalent halves of the ligand (Fig. 3).

In addition, in the solid state the *cis* isomer was the only species found in the unit cell. Single crystals suitable for X-ray analysis (colorless plates, $\sim 0.5\text{--}0.5\text{--}0.2\text{ mm}^3$ in size) were obtained by slow diffusion of *n*-hexane into a CD_2Cl_2 solution of **1a** at $T = 277\text{ K}$.

Compound **1a** crystallized in the $P2_1/a$ centrosymmetric monoclinic space group as a racemic mixture, with one complex molecule in the crystal asymmetric unit (Fig. 4). The pyridylbenzamidine moiety in structure **1a** chelates the metal center with the iminic N3 and the pyridinic N1 nitrogen atoms with a square planar coordination geometry as previously reported for the analogous complex dichlorido-(*N'*-(2,6-diisopropylphenyl)-4-methyl-*N*-(pyridin-2-yl)benzenecarboximidamide)-palladium [22]. The coordination geometry locked the pyridylbenzamidine ligand in an *E,syn,s-cis* conformation. For amidines the Δ_{CN} parameter, defined as $\Delta_{\text{CN}} = d(\text{C}-\text{N}) - d(\text{C}=\text{N})$, was introduced to assess the extent of delocalization within the “ $\text{--N}=\text{C}-\text{N}$ ” fragment [31,32]. For **1a** the Δ_{CN} of 0.085 \AA indicated a fully localized system and allowed us to locate proton H2 on N2 (Table 1), as confirmed by inspection of electron density maps during structure refinement. An analogous situation was reported for the unbound *N*-phenyl-*N'*-2-pyridylbenzamidine ligand, where N2 atom was fully protonated ($\Delta_{\text{CN}} = 0.12\text{ \AA}$) [34]. The bite angle N1-Pd-N3 of

$87.87(5)^\circ$ is very close to the value for an ideal square planar geometry. The dihedral angle between the square plane and the plane containing the *ortho*-substituted aryl ring of 86.5° indicates that the hindered aryl ring is orthogonal to the coordination plane, a key feature in catalysts for alkene polymerization (Fig. 4).

The crystal structure of **1a** can be almost perfectly superimposed onto the dichlorido variant [22]. The main difference between **1a** and the dichlorido complex is the replacement of a chlorido ligand with a methyl in **1a** coordination sphere. This substitution changes significantly the bond length between palladium and the pyridinic nitrogen N1 of the pyridylbenzamidine ligand, due to the *trans* influence of the methyl group (from $2.021(2)\text{ \AA}$ to $2.130(1)\text{ \AA}$ in **1a**) (Table 1).

When **1a** was reacted with silver hexafluorophosphate in the presence of acetonitrile under the reaction conditions typically applied for the halogen abstraction [37,38,18], the expected monocationic complex $[\text{Pd}(\text{CH}_3)(\text{CH}_3\text{CN})(\mathbf{1})][\text{PF}_6]$, **1b**, was obtained as a white solid (Scheme 3a). Its NMR characterization in CD_2Cl_2 solution was in agreement with the expected structure. Only one species was present in solution, but unlike the neutral derivative **1a**, the NOE experiment demonstrated that this species was the *trans* isomer, having the Pd- CH_3 moiety *trans* to the Pd- N_{iminio} bond (Fig. S19). Low temperature NMR experiments (up to 253 K) performed on the CD_2Cl_2 solutions of both **1a** and **1b** as well as ^1H NMR spectra recorded in CD_3NO_2 probed evidence of the presence of one isomer only for each complex.

Ligand **1** was reacted with the palladium precursor **5** under mild conditions leading to the isolation of a white solid that was characterized both in solid state, by X-ray analysis, and in CD_2Cl_2 solution, by NMR spectroscopy.

In the ^1H NMR spectrum the signals typical of ligand **1** and 1,5-cyclooctadiene, both coordinated to palladium, and of the Pd- CH_3 fragment were observed, while no resonance due to acetonitrile was present, thus indicating that the latter was replaced by the pyridylbenzamidine ligand. Whereas at room temperature, the signals of coordinated **1** were sharp, those of cod were broad and their decoalescence was reached at $T = 253\text{ K}$ showing four peaks for both the CH and the CH_2 protons, thus indicating that cod was

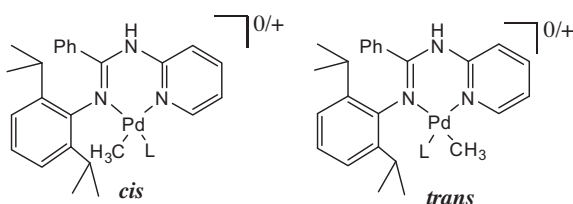


Fig. 3. The possible *cis* and *trans* isomers of **1a** and **1b** ($\text{L} = \text{Cl}^-$, CH_3CN).

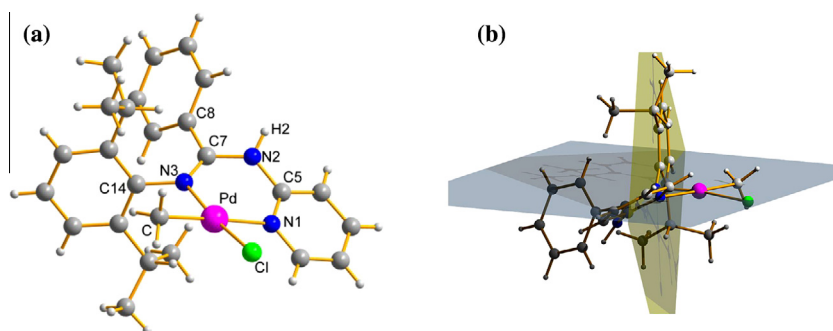


Fig. 4. X-ray structure of **1a** with: (a) labeling scheme for Pd coordination sphere (ball and stick representation); (b) the angle between the palladium coordination sphere (light gray) and the ligand 2,6-diisopropylphenyl substituent planes (yellow plane) is 86.5°. (For interpretation of the references to color in this figure legend, the reader is referred to the web version of this article.)

Table 1

Selected coordination distances (Å) and angles (°) for **1a** and **1c** (values averaged on the two ASU molecules (ASU = asymmetric unit)) complexes. 1,5-cyclooctadiene bond lengths and angles are reported as averages of values in *trans* (C^{C^T}) and *cis* (C^{C^C}) to palladium-methyl group. Complete table is available as [Supplementary Materials](#) (Tables S2 and S3).

Bond distances (Å)			
	1a		1c
Pd–C	2.053(2)	Pd–C	2.035(3)
Pd–N1	2.130(1)	Pd–N1	2.093(2)
Pd–N3	2.077(1)	Pd–C ^{C^C}	2.179(3)
Pd–Cl	2.339(1)	Pd–C ^{C^T}	2.349(3)
C7–N3	1.294(2)	C7–N3	1.349(3)
C7–N2	1.379(2)	C7–N2	1.306(4)
Δ_{CN}	0.085	Δ_{CN}	0.043
Bond angles (Å)			
	1a		1c
C–Pd–Cl	87.26(4)	C ^{C^C} –Pd–C	91.73(13)
C–Pd–N3	93.24(6)	C ^{C^C} –Pd–N1	93.58(10)
N1–Pd–Cl	91.85(4)	N1–Pd–C	88.44(11)
N1–Pd–N3	87.87(5)	C ^{C^C} –Pd–C ^{C^T}	86.46(12)

bonded to palladium in a nonsymmetric environment (Fig. 5). It is worthwhile to mention that both H³ and one of the protons of a CH₂ group of cod resonated at an unusually low frequency (6.22 ppm and 1.09 ppm, respectively), suggesting that they experienced a shielding cone. In addition, both the CH and the methyl groups of the isopropyl substituents, that at room temperature originated one signal each, at *T* = 253 K led to two different resonances, suggesting that the hindered rotation of dip was slowed down at low temperature.

On the basis of this NMR analysis the solid isolated from the reaction of **1** with **5** was formulated as [Pd(cod)(CH₃)(**1**)]PF₆, **1c** (Scheme 3b), with the cod ligand involved in a dynamic process at a rate intermediate on the NMR time scale, at room temperature.

The X-ray analysis of single crystals (colorless rods, ~0.3–0.4–0.2 mm³), grown by slow diffusion of diethyl ether in a CD₂Cl₂ solution of **1c** at *T* = 277 K, was in agreement with the structure depicted by the NMR data (Fig. 6).

Compound **1c** crystallized in the orthorhombic space group *Pbc*₂ with two complex and two diethyl ether solvent molecules in the ASU. The two crystallographically independent molecules in **1c** crystals were almost perfectly superimposable. It was a racemic mixture with crystals affected by inversion twinning. The palladium adopted a heavily distorted square pyramid geometry, with the pyridylbenzamidine ligand bonded to it in a monodentate fashion through the pyridinic N1 atom that fell in the plane containing the methyl and cyclooctadiene ligands, whereas the N2 atom occupied an apical position with a Pd···N2 distance of about

2.98 Å suggesting a weak interaction between these two atoms (Table S3). The coordination geometry locked the pyridylbenzamidine ligand in an *E,s-trans* conformation. Bond lengths related to the N2–C7–N3 fragment indicated a change in bond orders compared to **1a**, resulting in a tautomeric rearrangement that shifted the proton from N2 to N3. The Δ_{CN} value of 0.043 Å, smaller than in **1a**, indicated a lower degree of localization of these two bonds. The expected asymmetry for the coordinated cyclooctadiene was shown [34,42], which led to longer bond lengths for Pd–cod carbons *trans* to Pd–CH₃ group. The Pd–CH₃ bond distance, itself, was also affected by the nature of the donor atom *trans* to it, being remarkably shorter in **1c** than in **1a** (2.035(3) versus 2.053(2) Å, respectively).

Another significant difference among the structures of **1a** and **1c** is spotted on the 2,6-diisopropylphenyl substituent, which is perpendicular to the palladium coordination plane in the first case and almost parallel to it in the other model (Figs. 4b and 6b). This change in conformation is due to different steric hindrance of dip in the two coordination modes found (square planar and distorted square pyramid) and changes drastically the accessibility to the metal center in the two complexes, acting as a “cap” on the top face of the palladium square plane in **1c**. Finally, in the latter the plane containing the N2–C7–N3 fragment is almost orthogonal to the square plane (Fig. 6c).

By combining the solid state and the solution structures it was possible to explain some features of the NMR spectrum: the cod was coordinated in a nonsymmetric environment, thus generating different signals for each of its protons; the H³ of the pyridine ring fell in the shielding cone of the unsubstituted phenyl ring, thus it resonated at a low chemical shift; one of the protons of one of the CH₂ groups of cod experienced the shielding cone of dip upon it, thus it also resonated at a low chemical shift; finally, the two aryl rings were far away from each other and so at room temperature there was no restricted rotation of the substituted aryl ring around the N–dip bond. Moreover, the signal of the proton bonded to the nitrogen atom progressively shifted to low frequency going from the free ligand (13.18 ppm), to **1a** (7.44 ppm) to **1c** (6.88 ppm), thus suggesting that its chemical shift values might be used as a probe for the nature of the observed tautomer.

When the reaction of **1** with **5** was followed over time by reacting in the NMR tube a 10 mM dichloromethane solution of **5** with 1 equivalent of **1**, at room temperature, the species formed immediately after the mixing of the compounds was **1c**, which over time slowly evolved to **1b**, [Pd(CH₃)(CH₃CN)(**1**)]PF₆ with the dissociation of cod, the coordination of **1** as a bidentate ligand, while the acetonitrile reentered in the first coordination sphere of palladium (Figs. S25 and S26; Scheme 3b). However, even after 1 day **1c** remained the main species in solution.

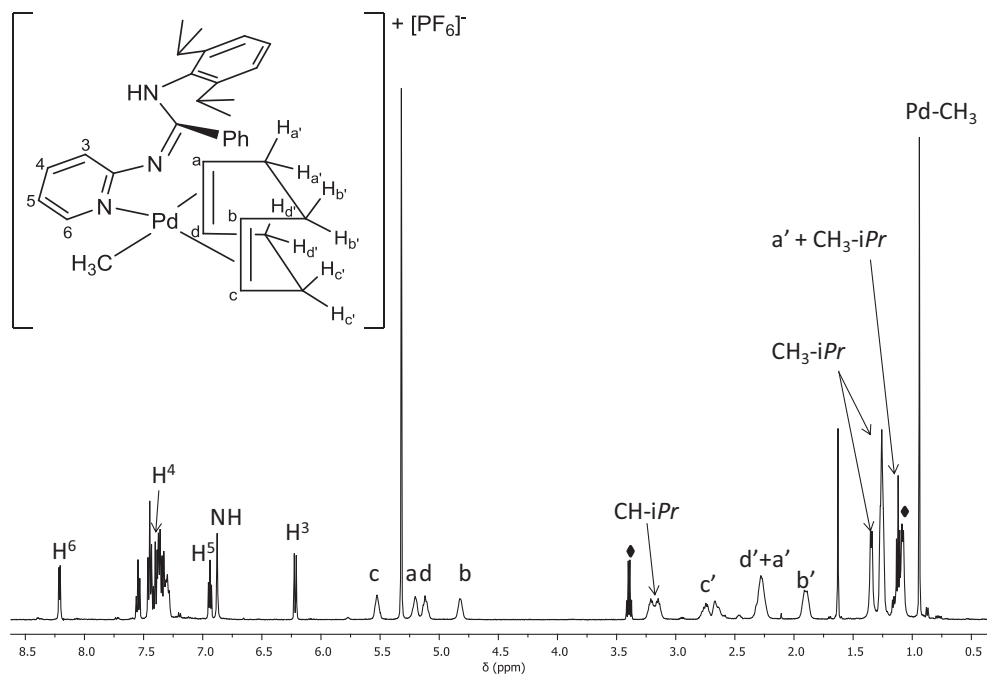


Fig. 5. ^1H NMR spectrum of **1c**, in CD_2Cl_2 , at 253 K, with the numbering scheme of the ligands. \blacklozenge Diethyl ether.

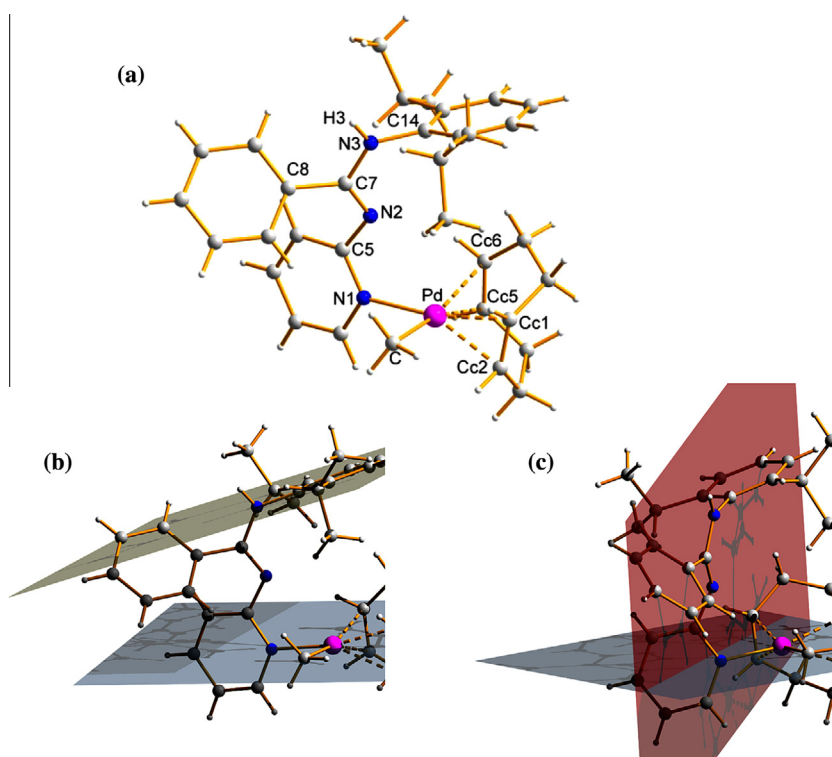


Fig. 6. X-ray structure of **1c** with: (a) labeling scheme for Pd coordination sphere (ball and stick representation); (b) the angle between palladium coordination sphere (light gray) and ligand 2,6-diisopropylphenyl substituent planes (yellow plane) is 16.5° ; (c) the angle between palladium coordination sphere (light gray) and ligand planes (containing N2, C7 and N3 – red plane) is 82° .

When ligands **2** and **3** were reacted with $[\text{Pd}(\text{cod})(\text{CH}_3)\text{Cl}]$ under the well established reaction conditions [37,18], no reaction took place (Scheme 3b). Instead, both ligands reacted with the palladium precursor **5** but leading to different complexes.

From the reaction of **2** with **5**, under the same conditions of ligand **1**, a white solid was isolated. In the ^1H NMR spectrum of

the solid in CDCl_3 , sharp signals were already observed at room temperature. They were analogous to those observed in the ^1H NMR spectrum of **1c** at 253 K indicating that the obtained product was $[\text{Pd}(\text{cod})(\text{CH}_3)(\mathbf{2})][\text{PF}_6]$, **2c** (Fig. S27). However, in contrast to **1c**, when the reactivity of **2** with **5** was studied by *in situ* NMR experiments, the immediate formation of **2c** was observed, but

no further transformation within 72 h occurred, thus indicating that **2c** was the only species formed and it did not transform to the corresponding $[\text{Pd}(\text{CH}_3)(\text{CH}_3\text{CN})(\mathbf{2})][\text{PF}_6]$ complex (Scheme 3b).

Upon slow diffusion of *n*-pentane into a CDCl_3 solution of **2c**, single crystals suitable for X-ray analysis were obtained (Figs. S1 and S2, Tables S2 and S3).

Compound **2c** crystallized, as a racemic mixture, in the monoclinic space group $P2_1/n$ with one complex molecule in the crystal asymmetric unit and with a centrosymmetric packing. Its crystal structure was the same as that observed for **1c**, with the nitrogen-donor ligand in its tautomeric form (the Δ_{CN} value was the same found for **1c**) and bonded to palladium in a monodentate fashion through the pyridinic nitrogen atom. The cyclooctadiene molecule was coordinated in a nonsymmetric way due to the *trans* influence of the $\text{Pd}-\text{CH}_3$ fragment *trans* to one C–C double bond (Fig. S1).

As found for **1c**, the structure of **2c** in solid state corresponded with the structure in solution.

Instead, no solid was isolated from the reaction of **3** with **5**. Thus, the latter reaction was studied by *in situ* NMR spectroscopy by adding almost 1 equivalent of **3** to a 10 mM CD_2Cl_2 solution of **5**, at room temperature. In the spectrum recorded immediately after mixing the two compounds, the signals of a new palladium species (I) together with those of free cyclooctadiene were observed, while no signal due to the free pyridylbenzamidine **3** was detected (Fig. 7). The reaction was followed with time, and in the spectrum recorded after 1 h the resonances of a second palladium species (II) were observed together with the singlet of methane (0.21 ppm). After one day, the first species formed disappeared in favor of the second one that became the major product (Figs. S31 and S32).

The first palladium complex formed (I) was identified as $[\text{Pd}(\text{CH}_3)(\text{CH}_3\text{CN})(\mathbf{3})][\text{PF}_6]$, **3b**, by full NMR characterization at 273 K to slow down its transformation into the second species. **3b** was detected as the *trans* isomer, featured by the $\text{Pd}-\text{CH}_3$ group *trans* to the $\text{Pd}-\text{N}_{\text{imino}}$ bond (Scheme 3b).

The nature of the second palladium species formed was unambiguously identified by NMR spectroscopy. The main evidences

from the NMR analysis were the integration of the doublets of the methyl groups of the isopropyl substituents corresponding to 9 instead of the expected 12 protons (Fig. 8), and the presence of a CH_2 fragment (Fig. S39), indicating that one of the two isopropyl substituents was transformed into a $\text{CH}_3(\text{CH})\text{CH}_2$ moiety, bonded to palladium, forming the six-membered metallacycle, **3d** (Scheme 3b).

The palladacycle **3d** was obtained from **3b** through the C–H activation of one methyl group of one of the two isopropyl substituents that gave its proton to the $\text{Pd}-\text{CH}_3$ fragment, originating methane that left the palladium coordination sphere. The fourth coordination site on the metal was occupied by the $\text{CH}_3(\text{CH})\text{CH}_2$ moiety. **3b** had the proper geometry for this reaction, having the acetonitrile, the more labile ligand, in *cis* to the substituted aryl ring. The activation of C–H bond of the *ortho* isopropyl substituents on the aryl ring of α -diimines was observed by Brookhart in $[\text{Pd}(\text{CH}_3)(\text{OEt}_2)(\text{iso-DAB})][\text{BARF}]$ having diethyl ether as labile ligand (OEt_2 = diethyl ether; iso-DAB = bis(2,6-diisopropylphenyl)-1,4-diaza-1,3-butadiene); $\text{BARF} = [\text{B}(3,5-(\text{CF}_3)_2\text{C}_6\text{H}_4)_4]$ [43], while the corresponding acetonitrile derivative was found to be stable for weeks in dichloromethane solution. In addition, the activation of C–H bonds of ligands having alkyl substituents in close proximity to palladium was reported for Pd(II) complexes with 2,2'-bipyridines bearing alkyl groups in *ortho* position with respect to the nitrogen-donor atoms [38,44,45].

2.3. Reactivity with ethylene of Pd(II) complexes **1b**, **1c**, **2c**

Complexes **1b**, **1c** and **2c** were tested as precatalysts for the ethylene/methyl acrylate copolymerization by carrying out the reaction in a glass pressure reactor, in 2,2,2-trifluoroethanol (TFE), at $T = 308$ K and $P_{\text{ethylene}} = 2.5$ bar, for 24 h. During the catalysis the formation of inactive palladium metal was evident. After the work up of the catalytic mixture only traces of palladium intermediates were obtained with no formation of the ethylene/MA copolymer and/or of higher alkenes. Notably, the GC–MS analysis of a small portion of the reaction mixture evidenced only the presence of very small amounts of butenes. This behavior is in contrast to that reported in the literature for the relevant Ni(II) complexes,

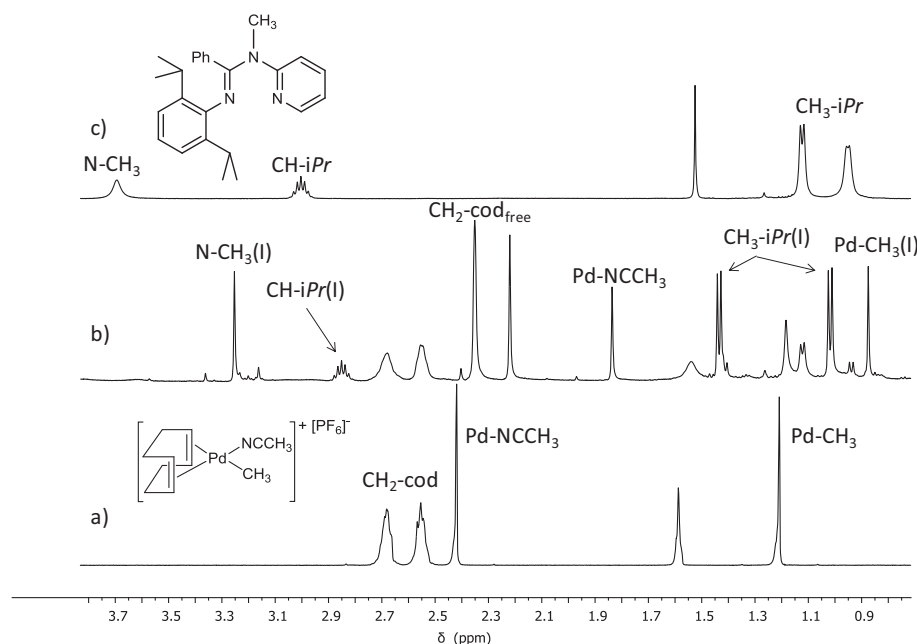


Fig. 7. ^1H NMR spectra in CD_2Cl_2 , at 298 K of: (a) **5**; (b) **5** + ~ 1 equiv. of **3**; (c) **3**. Region of aliphatic protons.

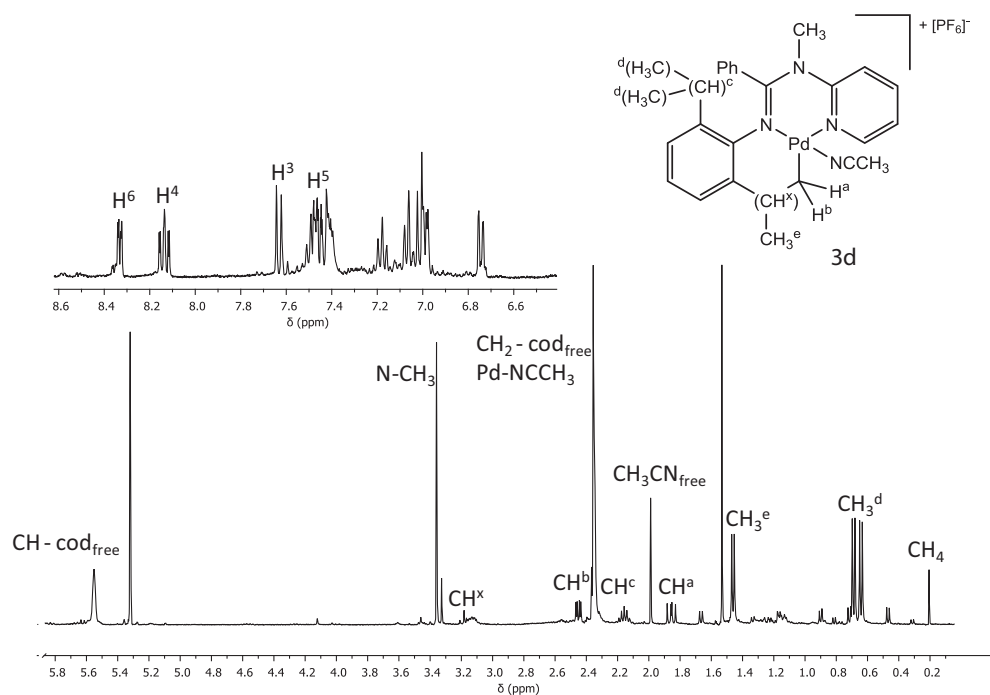


Fig. 8. ^1H NMR spectrum in CD_2Cl_2 , at 298 K of **5** + ~ 1 equiv. of **3** after 1 day.

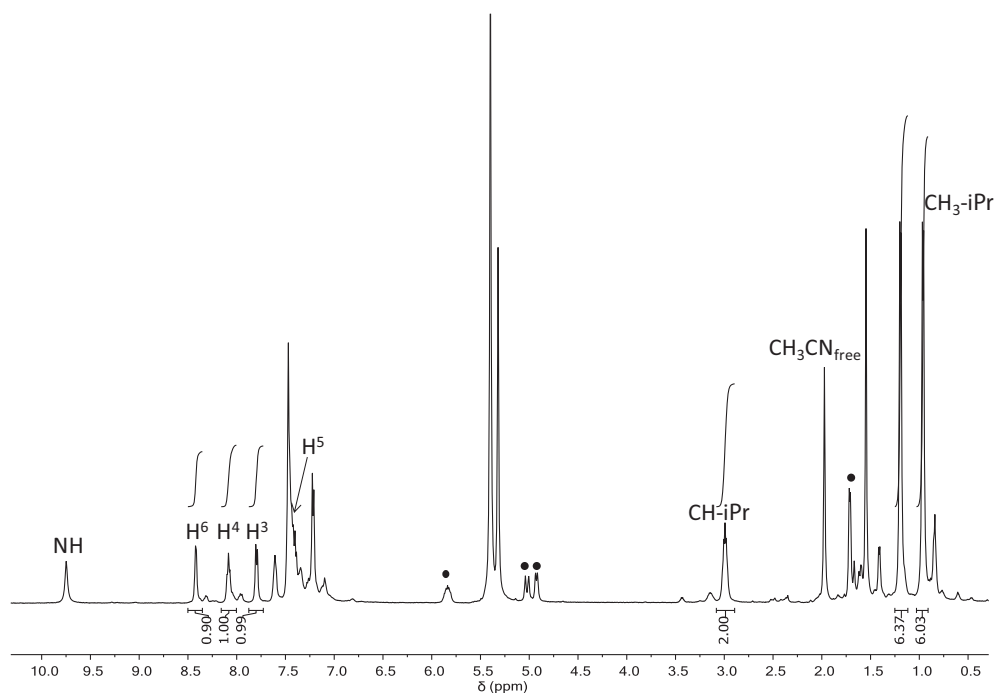


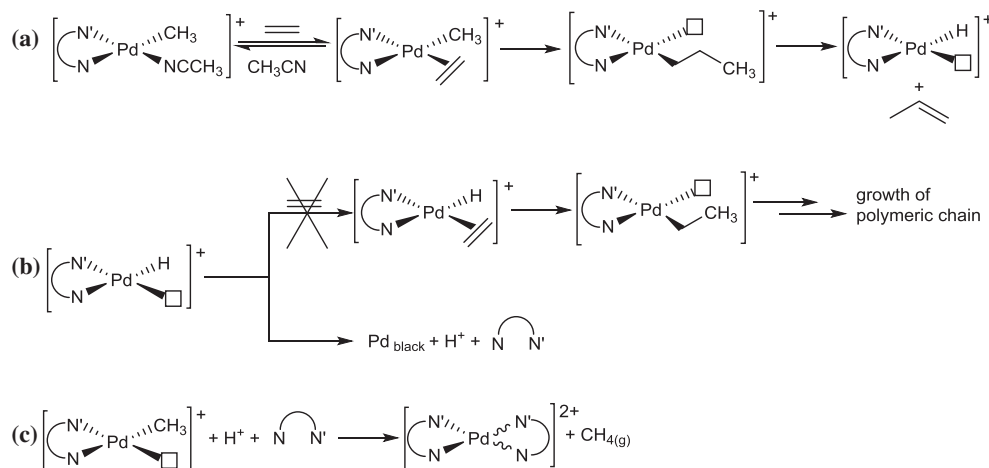
Fig. 9. ^1H NMR spectrum in CD_2Cl_2 , at 283 K of **1b** + ethylene at $t = 20$ min. ●Propylene.

that were found to be catalysts for ethylene oligomerization [23]. On the other hand, the formation of butenes in trace amount has been previously reported using Pd–carbene complexes having hindered substituents [46].

With the aim to understand the reason for the inactivity of these complexes, the reactivity of **1b** with the two comonomers, ethylene and methyl acrylate, was studied by *in situ* NMR experiments. The addition of 2 equivalents of MA to a CD_2Cl_2 solution of **1b**, at room temperature, did not result in either any coordination or migratory insertion of the polar monomer into the Pd–CH₃ bond,

thus demonstrating that the polar monomer had no tendency to substitute acetonitrile in the palladium coordination sphere, likely for steric reasons.

The reactivity with ethylene was studied by bubbling it into a CD_2Cl_2 solution of **1b** for 5 min, at room temperature. In the spectrum recorded immediately after the addition of the alkene, the signals of the precatalyst were still present together with the singlet of free acetonitrile and some new signals, including those of propene (Fig. S40). After 20 min the formation of palladium metal was evident, but no signal due to the free ligand was observed



Scheme 4. Proposed reaction mechanism for the reactivity of **1b** with ethylene.

and the ^1H NMR spectrum indicated that only traces of **1b** were present, together with a new palladium species identified as the dicationic, bischelated complex $[\text{Pd}(\mathbf{1})_2][\text{PF}_6]_2$ (Fig. 9). No resonance due to higher alkenes, like butenes, hexenes, etc., was observed.

On the basis of this NMR analysis it is possible to propose a hypothesis for the mechanism of the reaction between **1b** and ethylene. According to the literature [1], the activation reaction of the Pd-CH₃ precatalyst involves the alkene coordination to palladium through the substitution reaction of acetonitrile; afterwards its immediate migratory insertion into the Pd-CH₃ bond takes place, followed by the β -H elimination that leads to propene and to the Pd-hydride intermediate (Scheme 4a).

The Pd-hydride species is the real catalyst; on it the coordination and migratory insertion of ethylene can take place starting the growth of a polymeric chain. However, it also represents the starting point for catalyst deactivation. It may dissociate the hydrogen atom as a proton, leading to a Pd(0) intermediate that, by dissociation of the nitrogen-donor ligand, gives palladium black and the free ligand (Scheme 4b) [47].

With the precatalysts herein reported, in place of the resonances of the free ligand, those of the dicationic palladium complex $[\text{Pd}(\mathbf{1})_2][\text{PF}_6]_2$ were evident, thus indicating that an additional deactivation pathway is operative. For Pd(II) complexes with α -diimines applied as catalysts for both ethylene homopolymerization and ethylene/MA copolymerization, the formation of inactive dicationic species $[\text{Pd}(\text{N}-\text{N}')_2][\text{X}]_2$ has been recently proposed as a new deactivation pathway [16]. The mechanism is unclear, but it has been suggested to be a bimolecular process with one molecule of the palladium complex abstracting the ligand from another molecule to produce the dicationic species and palladium black. In the complexes under investigation, it is reasonable to assume that the proton and the pyridylbenzamidinium ligand dissociated from the Pd-H intermediate attack, respectively, the Pd-CH₃ bond, yielding methane, and the two so created vacant coordination sites of another precatalyst molecule (Scheme 4c).

3. Conclusions

In this paper we have investigated the coordination chemistry to Pd(II) of three pyridylbenzamidinium ligands, **1–3**, differing in the presence of a methyl group either on the pyridine ring or on the sp^3 nitrogen atom bridging the two moieties of the molecule. Ligand **3** is reported herein for the first time. An in-depth NMR study in solution probed evidence of the presence of several

equilibria among different isomers of the ligands, that might affect their coordinating capability. Indeed, despite their similarity, the three ligands show remarkably different coordinating behavior to Pd(II): **1** is able to act both as a bidentate and a monodentate ligand, in the latter mode it prefers its tautomeric form; **2** acts only as a monodentate ligand through its tautomer, suggesting that the introduction of one methyl group in position 6 of the pyridine ring encumbers too much the first coordination sphere of palladium to generate a stable square plane complex; **3** does not show the predicted coordinating behavior leading to a palladacycle through the C-H activation of one isopropyl group of dip, suggesting that the tautomerism, that is not possible due to the introduction of the methyl group on the sp^3 nitrogen, is of fundamental importance for the coordination to palladium.

Even though the structural features of the synthesized complexes, like two different N-donors, the six-membered palladacycle, the bridging nitrogen atom with a methyl group, the orthogonal orientation of the substituted aryl ring with respect to the square planar plane, were in favor of a catalytic activity, none of the tested complexes generated active species for either the ethylene/MA copolymerization or the ethylene homopolymerization. The *in situ* NMR investigation probed evidence that neither methyl acrylate nor ethylene were prone to give rise to their migratory insertion reaction into the Pd-alkyl bond. In fact, the activation of the precatalyst led to the Pd-hydride intermediate that evolved towards the inactive dicationic complex $[\text{Pd}(\text{N}-\text{N}')_2][\text{X}]_2$ instead of reacting with an incoming monomer molecule.

4. Experimental

4.1. General procedures and materials

All complex manipulations were performed using standard Schlenk techniques under argon. Anhydrous dichloromethane was obtained by distillation over CaH₂ under argon. Ligands **1** [23] and **2** [22], $[\text{Pd}(\text{CH}_3)\text{Cl}(\text{cod})]$ **4**, the neutral Pd complexes and the acetonitrile derivative were synthesized according to literature procedures [37]. $[\text{Pd}(\text{OAc})_2]$ was a donation from Engelhard Italia and used as received. Ethylene (purity $\geq 99.9\%$) supplied by SIAD and methyl acrylate (99.9%, with 0.02% of hydroquinone monomethyl ether) supplied by Aldrich were used as received. Deuterated solvents, Cambridge Isotope Laboratories, Inc., were stored as recommended by CIL. All the other reagents and solvents were purchased from Sigma-Aldrich and used without further purification for synthetic, spectroscopic and catalytic purposes.

NMR spectra of ligands, complexes, and of the *in situ* reactivity investigations were recorded on a Varian 500 spectrometer at the following frequencies: 500 MHz (^1H) and 125.68 MHz (^{13}C); the resonances are reported in ppm (δ) and referenced to the residual solvent peak versus $\text{Si}(\text{CH}_3)_4$: CDCl_3 at δ 7.26 (^1H) and δ 77.0 (^{13}C), CD_2Cl_2 at δ 5.32 (^1H) and δ 54.0 (^{13}C), CD_3NO_2 at 4.33 (^1H). NMR experiments were performed employing the automatic software parameters; in the case of NOESY experiments a mixing time of 500 ms was used.

IR spectra were recorded in Nujol on a Perkin Elmer System 2000 FT-IR. Elemental analyses were performed in the analytical laboratories of Department of Chemistry of University of Bologna. GC-MS analysis of the possible products of cooligomerization were performed using a Agilent 7890 GC equipped with a 5975C mass spectrometer. The separation was achieved with a DB-225 ms column (30 m, ID 0.25 mm, 0.25 μm film) using He as carrier. For the analysis, a small portion (200 μL) of solution after cooligomerization experiments was diluted with MeOH (1 mL).

4.2. Synthesis of ligands 1–3

N-(2,6-diisopropyl)phenyl-*N'*-2-pyridylbenzamidinium **1** was prepared according to the literature [23] and was obtained as a yellow solid in a 45% yield.

^1H NMR (500 MHz, CD_2Cl_2 , 298 K) δ = 13.18 (s, 1H, NH), 8.29 (d, 1H, H⁶), 7.70 (m, 1H, H⁴), 7.40 (d, 1H, Ph), 7.26 (m, 1H, H³), 7.20–7.08 (m and br signals, 7H, ArH), 6.95 (m, 1H, H⁵), [3.25 (m, CH-*iPr*), 3.04 (m, CH-*iPr*) total area 2H], [1.13 (d, CH₃-*iPr*), 0.94 (d, CH₃-*iPr*), total area 12H].

^{13}C NMR (125.68 MHz, CD_2Cl_2 , 298 K) δ = 29.12 (CH-*iPr*), 28.74 (CH-*iPr*), 24.85 (CH₃-*iPr*), 21.69 (CH₃-*iPr*).

ESI-MS 381.1 [MH+Na]⁺, 358.1 [MH]⁺, 264.0 [M–PyNH]⁺.

N-(2,6-diisopropyl)phenyl-*N'*-(6-methyl)-2-pyridylbenzamidinium **2** was prepared according to the literature [22] and was obtained as a yellow solid in a 50% yield.

^1H NMR (500 MHz, CD_2Cl_2 , 298 K) δ = 13.28 (br, 1H, NH), 7.62 (bt, 1H, H⁴), 7.40–7.15 (m and br signals, 7H, ArH) 7.09 (m, 1H, H³), 6.84 (d, 1H, H⁵), [3.28 (m, CH-*iPr*), 3.04 (m, CH-*iPr*) total area 2H], 2.46 (s and br, 3H, Py-CH₃), [1.14 (2d, CH₃-*iPr*), 0.96 (d, CH₃-*iPr*), total area 12H].

^{13}C NMR (125.68 MHz, CD_2Cl_2 , 298 K) δ = 138.32 (4-C_{py}), 123.82 (3-C_{py}), 117.44 (5-C_{py}), 28.99 (CH-*iPr*), 28.68 (CH-*iPr*), 24.20 (Py-CH₃), 25.52 (CH₃-*iPr*), 24.38 (CH₃-*iPr*), 21.85 (CH₃-*iPr*).

ESI-MS 394.1 [M+Na]⁺, 372.1 [M+H]⁺, 264.0 [M–Py(CH₃)NH]⁺.

N-(2,6-diisopropyl)phenyl-*N'*-methyl-*N'*-2-pyridylbenzamidinium **3**.

2-(*N*-methylamino)pyridine was prepared according to the literature [28].

To a 10 mL THF solution of the intermediate imidoylchloride [23] (0.6 g, 2.0 mmol) and 2-(*N*-methylamino)pyridine (0.21 g, 2.0 mmol), NaH (0.16 g, 4.0 mmol, 60% dispersion in mineral oil) was added portionwise at -10°C under inert atmosphere. After the addition was complete, the mixture was left stirring to reach the room temperature, then heated to reflux for 7 h. The course of the reaction was monitored by TLC (petroleum ether/ethyl acetate 8:2). After consumption of the amine, CH_2Cl_2 was added (20 mL) and the solution extracted with dil. HCl (10 mL).

The organic layer was dried (Na_2SO_4), and the solvent removed under reduced pressure to give an oil which was purified on column removing also the mineral oil (eluent: petroleum ether/ethyl acetate 98/2).

Ligand **3** was obtained as a yellow solid in a 30% yield.

^1H NMR (500 MHz, CD_2Cl_2 , 263 K) δ = 8.27 (dd, 1H, H⁶), 7.30 (td, 1H, H⁴), 7.09–6.99 (m, 5H, aromatic H), 6.93–6.91 (m, 2H, aromatic H), 6.88–6.85 (m, 1H, aromatic H), 6.82–6.80 (m, broad, 1H, H⁵),

6.61 (d, 1H, H³), 3.69 (s, 3H, N-CH₃), 2.97 (m, 2H, CH-*iPr*), 1.11 (d, 6H, CH₃-*iPr*), 0.90 (d, 6H, CH₃-*iPr*).

^{13}C NMR (125.68 MHz, CD_2Cl_2 , 298 K) δ = 138.32 (4-C_{py}), 123.82 (3-C_{py}), 117.44 (5-C_{py}), 28.99 (CH-*iPr*), 28.68 (CH-*iPr*), 24.20 (Py-CH₃), 25.52 (CH₃-*iPr*), 24.38 (CH₃-*iPr*), 21.85 (CH₃-*iPr*).

ESI-MS 394.2 [M+Na]⁺, 372.1 [M+H]⁺, 264.1 [M–PyNH]⁺.

4.3. Synthesis of Pd(II) complexes

4.3.1. Synthesis of [Pd(cod)(CH₃)(CH₃CN)][PF₆], **5**

To a solution of 0.26 mmol (70 mg) of [Pd(cod)(CH₃Cl)], **4**, in 2 mL anhydrous dichloromethane in a Schlenk tube under inert atmosphere, a solution of AgPF₆ (1.2 equiv., 80.5 mg, 0.32 mmol) in 2 mL of anhydrous acetonitrile was added under stirring. The reaction mixture was protected from light and stirred for 1 h, then it was filtered over Celite®; the desired solid was precipitated from the mother liquor upon addition of diethyl ether, then filtered, washed thoroughly with diethyl ether and dried under vacuum. Yield: 60%.

IR: ν_{max} = 844.08 cm⁻¹ (PF₆⁻). Anal. Calc. for PdC₁₁H₁₈NPF₆: C, 31.79; H, 4.16; N, 3.27. Found: C, 31.58; H, 4.12; N, 3.13%.

^1H NMR (500 MHz, CD_2Cl_2 , 298 K) δ = 5.88 (broad, 2H, CH-cod), 5.43 (broad, 2H, CH-cod), 2.68 (broad, 4H, CH₂-cod), 2.55 (broad, 4H, CH₂-cod), 2.42 (s, 3H, Pd-NCCH₃), 1.21 (s, 3H, Pd-CH₃).

^{13}C NMR (500 MHz, CDCl_3 , 298 K): δ = 123.96 (CH-cod), 104.53 (CH-cod), 30.78 (CH₂-cod), 27.72 (CH₂-cod), 13.15 (Pd-CH₃), 2.97 (Pd-NCCH₃).

4.3.2. Synthesis of [Pd(**1**)(CH₃)Cl], **1a**

To a stirred solution of [Pd(CH₃)Cl(cod)] (0.36 mmol) in dichloromethane (1 mL), a solution of ligand **1** (1.1 equiv.) in dichloromethane (2 mL) was added. After 5 h of stirring at room temperature, the reaction mixture was concentrated and the product precipitated upon addition of cold diethyl ether. Yield: 74%.

Anal. Calc. for PdC₂₅H₃₀N₃Cl: C, 58.37; H, 5.98; N, 7.97. Found: C, 58.24; H, 6.02; N, 7.76%.

^1H NMR (500 MHz, CD_2Cl_2 , 298 K) δ = 9.44 (d, 1H, H⁶), 7.78 (m, 1H, H⁴), 7.44 (s, 1H, NH), 7.35–7.25 (aromatic H), 7.15 (m, 1H, H⁵), 7.1–6.95 (aromatic H), 6.94 (d, 1H, H³), 3.33 (m, 2H, CH-*iPr*), 1.39 (d, 6H, CH₃-*iPr*), 0.82 (d, 6H, CH₃-*iPr*), 0.14 (s, 3H, Pd-CH₃).

^{13}C NMR (125.68 MHz, CD_2Cl_2 , 298 K) δ = 150.3 (6-C_{py}), 139.57 (4-C_{py}), 127.77 (5-C_{py}), 114.20 (3-C_{py}), 28.30 (CH-*iPr*), 24.18 (CH₃-*iPr*), 23.56 (CH₃-*iPr*), 2.13 (Pd-CH₃).

^1H NMR (500 MHz, CD_3NO_2 , 298 K) δ = 9.35 (d, 1H, H⁶) 8.25 (s, 1H, NH), 7.88 (m, 1H, H⁴), 7.40–7.28 (aromatic H), 7.17 (m, 1H, H⁵), 7.12 (d, 1H, H³), 7.07–7.04 (aromatic H), 3.41 (m, 2H, CH-*iPr*), 1.40 (d, 6H, CH₃-*iPr*), 0.90 (d, 6H, CH₃-*iPr*), 0.05 (s, 3H, Pd-CH₃).

4.3.3. Synthesis of [Pd(**1**)(CH₃)(CH₃CN)][PF₆], **1b**

To a solution of 0.14 mmol (70 mg) of **1a** in 8 mL anhydrous dichloromethane in a Schlenk tube under inert atmosphere, a solution of AgPF₆ (1.2 equiv., 41.7 mg, 0.16 mmol) in 1.5 mL of anhydrous acetonitrile was added under stirring. The reaction mixture was protected from light and stirred for 1 h, then filtered over Celite®; the desired solid was precipitated from the mother liquor upon addition of diethyl ether, then filtered, washed thoroughly with diethyl ether and dried under vacuum. Yield: 60%.

IR: ν_{max} = 844.08 cm⁻¹ (PF₆⁻). Anal. Calc. for PdC₂₇H₃₃N₄PF₆: C, 48.77; H, 5.00; N, 8.23. Found: C, 48.61; H, 5.11; N, 8.19%.

^1H NMR (500 MHz, CD_2Cl_2 , 298 K) δ = 8.30 (d, 1H, H⁶), 8.08 (s, 1H, NH), 7.96 (m, 1H, H⁴), 7.45 (aromatic H), 7.35 (m, 1H, H³), 7.25 (aromatic H), 7.18 (m, 1H, H⁵), 7.15–7.00 (aromatic H), 3.16 (m, 2H, CH-*iPr*), 1.67 (s, 3H, Pd-NCCH₃), 1.41 (d, 6H, CH₃-*iPr*), 0.84 (m, 9H, CH₃-*iPr* + Pd-CH₃).

^{13}C NMR (125.68 MHz, CD_2Cl_2 , 298 K) δ = 150.07 (6- C_{py}), 141.60 (4- C_{py}), 129.69 (3- C_{py}), 120.93 (5- C_{py}), 28.86 (CH-*iPr*), 25.04 (CH₃-*iPr*), 23.55 (CH₃-*iPr*), 2.69 (Pd-NCCH₃), 2.21 (Pd-CH₃).

^1H NMR (500 MHz, CD_3NO_2 , 298 K) δ = 8.48 (s, 1H, NH), 8.41 (d, 1H, H⁶), 8.02 (m, 1H, H⁴), 7.47–7.37 (aromatic H), 7.30 (m, 1H, H³), 7.25 (m, 1H, H⁵), 7.17 (aromatic H), 3.28 (m, 2H, CH-*iPr*), 1.79 (s, 3H, Pd-NCCH₃), 1.46 (d, 6H, CH₃-*iPr*), 0.90 (d, 6H, CH₃-*iPr*), 0.84 (s, 3H, Pd-CH₃).

4.3.4. Synthesis of [Pd(cod)(CH₃)(N-N')][PF₆], **1c**, **2c**

0.18 mmol (75 mg) of **5** were dissolved in 8 mL anhydrous dichloromethane in a Schlenk tube under inert atmosphere; a solution of 1.2 equiv. of ligand (0.20 mmol; ligand **1** for **1c**, ligand **2** for **2c**) in 3 mL of anhydrous dichloromethane was added under stirring. The reaction mixture was protected from light and stirred for 40 min, then the desired solid was precipitated upon addition of diethyl ether, after which it was filtered, washed thoroughly with diethyl ether and dried under vacuum. Average yield: 80%.

1c – IR: ν_{max} = 844.08 cm^{-1} (PF₆⁻). Anal. Calc. for PdC₃₃H₄₂N₃PF₆: C, 55.24; H, 5.98; N, 5.64. Found: C, 55.36; H, 6.01; N, 5.61%.

^1H NMR (500 MHz, CD_2Cl_2 , 253 K) δ = 8.22 (d, 1H, H⁶), 7.55–7.33 (aromatic H), 7.34 (m, 1H, H⁴), 6.94 (m, 1H, H⁵), 6.88 (s, 1H, NH), 6.22 (d, 1H, H³), 5.53 (broad, 1H, CH^c-cod), 5.20 (broad, 1H, CH^a-cod), 5.12 (broad, 1H, CH^d-cod), 4.83 (broad, 1H, CH^b-cod), 3.18 (broad, 2H, CH-*iPr*), 2.74 (broad, 2H, CH₂^c-cod), 2.28 (broad, 3H, CH₂^{d+a'}-cod), 1.91 (broad, 2H, CH₂^b-cod), 1.34 (d, 3H, CH₃-*iPr*), 1.26 (m, 6H, CH₃-*iPr*), 1.09 (m, 4H, CH₂^c-cod + CH₃-*iPr*), 0.94 (s, 3H, Pd-CH₃).

^{13}C NMR (125.68 MHz, CD_2Cl_2 , 253 K) δ = 148.77 (6- C_{py}), 122.96 (CH^d-cod), 122.59 (CH^a-cod), 119.63 (3- C_{py}), 118.79 (5- C_{py}), 107.10 (CH^c-cod), 100.41 (CH^b-cod), 32.20–32.16 (CH₂^c-cod), 29.07 (CH-*iPr*), 28.96 (CH₂^b-cod), 28.74 (CH₂^b-cod), 27.20–26.71 (CH₂^c-cod), 25.18–22.06 (CH₃-*iPr*), 9.98 (Pd-CH₃).

2c – IR: ν_{max} = 844.08 cm^{-1} (PF₆⁻). Anal. Calc. % for PdC₃₄H₄₄N₃PF₆: C, 53.43; H, 5.98; N, 5.33. Found: C, 53.47; H, 5.90; N, 5.29%.

^1H NMR (500 MHz, CDCl_3 , 298 K) δ = 7.53–7.28 (m, 8H, Ph), 7.28 (1H, H⁴), 6.87 (d, 1H, H⁵), 6.75 (br, 1H, NH), 6.05 (d, 1H, H³), 5.65 (m, 1H, CH^c-cod), 5.30 (m, 1H, CH^a-cod), 5.10 (m, 1H, CH^d-cod), 4.78 (m, 1H, CH^b-cod), 3.28 (m, 1H, CH-*iPr* (I)), 3.17 (m, 1H, CH-*iPr* (II)), 2.86 (m, 4H, Py-CH₃ + CH₂^c-cod), 2.73 (m, 1H, CH₂^c-cod), 2.33 (m, 3H, CH₂^{d+ab}-cod), 1.90 (m, 2H, CH₂^b-cod), 1.40 (d, 3H, CH₃-*iPr* (II)), 1.30 (d, 6H, CH₃-*iPr* (I + II)), 1.15 (d, 3H, CH₃-*iPr* (I) + CH₂^c-cod), 0.99 (s, 3H, Pd-CH₃).

^{13}C NMR (125.68 MHz, CDCl_3 , 298 K) δ = 139.42 (4- C_{py}), 131.71–124.07 (Ph), 123.00 (CH^a-cod), 122.52 (CH^d-cod), 119.05 (5- C_{py}), 116.19 (3- C_{py}), 106.82 (CH^c-cod), 99.82 (CH^b-cod), 32.81 + 32.67 (CH₂^c-cod), 29.39 (CH-*iPr* (II)), 28.91 (CH-*iPr* (I)), 28.51 (CH₂^b-cod), 28.16 (CH₂^{a+ab}-cod), 27.46 (CH₂^b-cod), 26.23 (CH₃-Py), 26.07 (CH₂^d-cod), 25.35 + 22.27 (CH₃-*iPr* (I + II)), 24.07 (CH₃-*iPr* (II)), 22.30 (CH₃-*iPr* (I)), 8.62 (Pd-CH₃).

4.4. In situ reactivity of ligand **3** with [Pd(cod)(CH₃)(CH₃CN)][PF₆], **5**

To a 10 mM solution of complex **5** (0.008 mmol, 3.32 mg) in 0.80 mL CD_2Cl_2 in NMR tube, 1 equiv. of ligand **3** (0.008 mmol, 2.97 mg) was added at room temperature. The reaction was followed with time via NMR.

3b – ^1H NMR (500 MHz, CD_2Cl_2 , 273 K) δ = 8.33 (m, 1H, H⁶), 8.11 (m, 1H, H⁴), 7.5–6.8 (aromatic H), 7.41 (d, 1H, H³), 7.29 (m, 1H, H⁵), 3.23 (s, 3H, N-CH₃), 2.83 (sept, 2H, CH-*iPr*), 1.82 (s, 3H, Pd-NCCH₃), 1.41 (d, 6H, CH₃-*iPr*), 1.00 (d, 6H, CH₃-*iPr*), 0.84 (s, 3H, Pd-CH₃).

^{13}C NMR (125.68 MHz, CD_2Cl_2 , 273 K) δ = 151.04 (6- C_{py}), 141.78 (4- C_{py}), 115.53 (3- C_{py}), 41.85 (N-CH₃), 28.58 (CH-*iPr*), 2.92 (Pd-NCCH₃), 24.74 (CH₃-*iPr*), 23.28 (CH₃-*iPr*), 2.85 (Pd-CH₃).

3d – ^1H NMR (500 MHz, CD_2Cl_2 , 298 K) δ = 8.32 (m, 1H, H⁶), 8.13 (m, 1H, H⁴), 7.62 (d, 1H, H³), 7.45 (m, 1H, H⁵), 7.4–6.7 (aromatic H), 3.36 (s, 3H, N-CH₃), 3.12 (m, 1H, CH^x), 2.46 (m, 1H, CH^b), 2.35

(s, 3H, Pd-NCCH₃), 2.16 (m, 1H, CH^c), 1.85 (m, 1H, CH^a), 1.46 (d, 3H, CH₃^f), 0.69 (d, 3H, CH₃^g), 0.64 (d, 3H, CH₃^h).

^{13}C NMR (125.68 MHz, CD_2Cl_2 , 298 K) δ = 148.71 (6- C_{py}), 141.62 (4- C_{py}), 116.07 (3- C_{py}), 123.13 (5- C_{py}), 41.10 (CH^b), 3.61 (Pd-NCCH₃), 18.13 (CH₃^f), 24.08 (CH₃^g), 20.23 (CH₃^h).

4.5. Crystallographic data of complexes **1a**, **1c** and **2c**

Data collections were performed at the X-ray diffraction beamline (XRD1) of the Elettra Synchrotron, Trieste (Italy), with a Pilatus 2 M image plate detector. Complete datasets were collected at 100 K (nitrogen stream supplied through an Oxford Cryostream 700) with a monochromatic wavelength of 0.700 Å through the rotating crystal method. The crystals of **1a** ([Pd(**1**)(CH₃)Cl]), **1c** ([Pd(**1**)(cod)(CH₃)]PF₆) and **2c** ([Pd(**2**)(cod)(CH₃)]PF₆) were dipped in N-paratone and mounted on the goniometer head with a nylon loop. The diffraction data were indexed, integrated and scaled using XDS [48]. A complete dataset for the monoclinic crystal forms of compound **1a** was obtained by merging two different data collections done on the same crystal with different orientations. The structures were solved by direct methods using SIR2011 [49], Fourier analyzed and refined by the full-matrix least-squares based on F² implemented in SHELXL-2013 [50]. The Coot program was used for modeling [51]. Anisotropic thermal motion modeling was then applied to all atoms and hydrogen atoms were included at calculated positions with isotropic Ufactors = 1.2 Ueq or Ufactors = 1.5 Ueq for methyl groups. The structure of **1c** has been refined as an inversion twin, and disorder on PF₆⁻ counterion has been modeled. Essential crystal and refinement data (Table S1), together with selected bond distances and angles, are reported in the manuscript and in Supplementary Materials (Tables 1, S2 and S3).

4.6. Ethylene/methyl acrylate copolymerization

All catalytic experiments were carried out in a Büchi “tinyclave” reactor equipped with an interchangeable 50 mL glass vessel. The vessel was loaded with the desired complex (21 μmol), TFE (21 mL) and methyl acrylate (1.13 mL). The reactor was then placed in a preheated oil bath, connected to the ethylene tank and pressurized. The reaction mixture was stirred at constant temperature and pressure. After 24 h, the reactor was cooled to room temperature and vented. An aliquot (200 μL) of the reaction mixture was withdrawn and diluted in CH₃OH (1 mL) for GC–MS analyses. The reaction mixture was poured in a 50 mL round flask, together with the dichloromethane (3 × 2 mL) used to wash the glass vessel. Volatiles were removed under reduced pressure and the residual oil was dried at constant weight and analyzed by NMR spectroscopy.

4.7. In situ reactivity of complex **1b** with ethylene

In a 10 mM solution of complex **1b** in CD_2Cl_2 in NMR tube, ethylene was bubbled for 5 min, then a ^1H NMR spectrum was recorded at 298 K immediately after mixing and after 20 min.

^1H NMR (500 MHz, CD_2Cl_2 , 298 K) δ = 9.67 (s, 1H, NH), 8.35 (d, 1H, H⁶), 8.01 (t, 1H, H⁴), 7.72 (d, 1H, H³), 7.53 (t, 1H, H⁵), 2.91 (sept, 2H, CH-*iPr*), 1.12 (d, 6H, CH₃-*iPr*), 0.89 (d, 6H, CH₃-*iPr*).

Acknowledgements

This work was financially supported by Università degli Studi di Trieste – Finanziamento di Ateneo per progetti di ricerca scientifica – FRA 2011, FRA 2012 and FRA 2013. Fondazione CRTrieste and Fondazione Benefica Kathleen Foreman Casali are gratefully acknowledged for the generous donations of a Varian 500 MHz spectrometer and a Büchi tinyclave glass reactor, respectively.

Appendix A. Supplementary material

CCDC 1015153, 1015009 and 1015008 contain the supplementary crystallographic data for complexes **1a**, **1c** and **2c**, respectively. These data can be obtained free of charge from The Cambridge Crystallographic Data Centre via www.ccdc.cam.ac.uk/data_request/cif. Supplementary data associated with this article can be found, in the online version, at <http://dx.doi.org/10.1016/j.ica.2015.01.049>.

References

- [1] L.K. Johnson, C.M. Killian, M. Brookhart, *J. Am. Chem. Soc.* 117 (1995) 6414.
- [2] S.D. Ittel, L.K. Johnson, M. Brookhart, *Chem. Rev.* 100 (2000) 1169.
- [3] V.C. Gibson, S.K. Spitzmesser, *Chem. Rev.* 103 (2003) 283.
- [4] A. Nakamura, S. Ito, K. Nozaki, *Chem. Rev.* 109 (2009) 5215.
- [5] A. Berkefeld, S. Mecking, *Angew. Chem., Int. Ed.* 47 (2008) 2538.
- [6] A. Sen, S. Borkar, *J. Organomet. Chem.* 692 (2007) 3291.
- [7] J.-Y. Dong, Y. Hu, *Coord. Chem. Rev.* 250 (2006) 47.
- [8] L.S. Boffa, B.M. Novak, *Chem. Rev.* 100 (2000) 1479.
- [9] S. Ito, K. Nozaki, *Chem. Rec.* 10 (2010) 315.
- [10] N.M.G. Franssen, J.N.H. Reek, B. de Bruin, *Chem. Soc. Rev.* 42 (2013) 5809.
- [11] A. Nakamura, T.M.J. Anselment, J. Claverie, B. Goodall, R.F. Jordan, S. Mecking, B. Rieger, A. Sen, P.W.N.M. van Leeuwen, K. Nozaki, *Acc. Chem. Res.* 46 (2013) 1438.
- [12] B.P. Carrow, K. Nozaki, *Macromolecules* 47 (2014) 2541.
- [13] L.K. Johnson, S. Mecking, M. Brookhart, *J. Am. Chem. Soc.* 118 (1996) 267.
- [14] S. Mecking, L.K. Johnson, L. Wang, M. Brookhart, *J. Am. Chem. Soc.* 120 (1998) 888.
- [15] C.S. Popeney, D.H. Camacho, Z. Guan, *J. Am. Chem. Soc.* 129 (2007) 10062.
- [16] L. Guo, H. Gao, Q. Guan, H. Hu, J. Deng, J. Liu, F. Liu, Q. Wu, *Organometallics* 31 (2012) 6054.
- [17] V. Rosar, A. Meduri, T. Montini, F. Fini, C. Carfagna, P. Fornasiero, G. Balducci, E. Zangrando, B. Milani, *ChemCatChem* 6 (2014) 2403.
- [18] A. Meduri, T. Montini, F. Ragaini, P. Fornasiero, E. Zangrando, B. Milani, *ChemCatChem* 5 (2013) 1170.
- [19] A. Scarel, M.R. Axet, F. Amoroso, F. Ragaini, C.J. Elsevier, A. Holuigue, C. Carfagna, L. Mosca, B. Milani, *Organometallics* 27 (2008) 1486.
- [20] F. Amoroso, E. Zangrando, C. Carfagna, C. Muller, D. Vogt, M. Hagar, F. Ragaini, B. Milani, *Dalton Trans.* 42 (2013) 14583.
- [21] A. Schatz, A. Scarel, E. Zangrando, L. Mosca, C. Carfagna, A. Gissibl, B. Milani, O. Reiser, *Organometallics* 25 (2006) 4065.
- [22] Y.-T. Huang, X. Tang, Y. Yang, D.-S. Shen, C. Tan, F.-S. Liu, *Appl. Organomet. Chem.* 26 (2012) 701.
- [23] F.-S. Liu, H.-Y. Gao, K.-M. Song, L. Zhang, F.-M. Zhu, Q. Wu, *Polyhedron* 28 (2009) 1386.
- [24] A.J. Swarts, F. Zheng, V.J. Smith, E. Nordlander, S.F. Mapolie, *Organometallics* 33 (2014) 2247.
- [25] A.J. Swarts, S.F. Mapolie, *Dalton Trans.* 43 (2014) 9892.
- [26] J.-A. Gautier, M. Miocque, C.C. Farnoux, *The Chemistry of Amidines and Imidates*, in: S. Patai (Ed.), vol. 1, Wiley, London, 1975, p. 283. Chapter 7.
- [27] G.V. Boyd, *The Chemistry of Amidines and Imidates*, in: S. Patai, Z. Rappoport (Eds.), vol. 2, Wiley, Chichester, 1991, p. 339. Chapter 7.
- [28] O.M. Singh, S.J. Singh, S.N. Kim, S.-G. Lee, *Bull. Korean Chem. Soc.* 28 (2007) 115.
- [29] M. Glos, O. Reiser, *Org. Lett.* 2 (2000) 2045.
- [30] G. Hafelinger, F.H. Kuske, *The Chemistry of Amidines and Imidates*, in: S. Patai, Z. Rappoport (Eds.), vol. 2, Wiley, Chichester, 1991. Chapter 1.
- [31] R.T. Boeré, V. Klassen, G. Wolmershäuser, *J. Chem. Soc., Dalton Trans.* (1998) 4147.
- [32] M.P. Coles, *Dalton Trans.* (2006) 985.
- [33] C.H. Perrin, *The Chemistry of amidines and imidates*, in: S. Patai, Z. Rappoport (Eds.), vol. 2, Wiley, Chichester, 1991. Chapter 3.
- [34] F.A. Cotton, P. Lei, C.A. Murillo, L.-S. Wang, *Inorg. Chim. Acta* 349 (2003) 165.
- [35] R.E. Rulke, J.G.P. Delis, A.M. Groot, C.J. Elsevier, P.W.N.M. van Leeuwen, K. Vrieze, K. Goubitz, H. Schenk, *J. Organomet. Chem.* 508 (1996) 109.
- [36] P. Burger, J. Baumeister, *J. Organomet. Chem.* 575 (1999) 214.
- [37] J. Durand, E. Zangrando, M. Stener, G. Fronzoni, C. Carfagna, B. Binotti, P.C.J. Kamer, C. Muller, M. Caporali, P.W.N.M. van Leeuwen, D. Vogt, B. Milani, *Chem. Eur. J.* 12 (2006) 7639.
- [38] A. D'Amora, L. Fanfoni, D. Cozzula, N. Guidolin, E. Zangrando, F. Felluga, S. Gladiali, F. Benedetti, B. Milani, *Organometallics* 29 (2010) 4472.
- [39] R.E. Rülke, J.M. Ernsting, A.L. Spek, C.J. Elsevier, P.W.N.M. Van Leeuwen, K. Vrieze, *Inorg. Chem.* 32 (1993) 5769.
- [40] A. Bastero, A. Ruiz, C. Claver, B. Milani, E. Zangrando, *Organometallics* 21 (2002) 5820.
- [41] M.R. Axet, F. Amoroso, G. Bottari, A. D'Amora, E. Zangrando, F. Faraone, D. Drommi, M. Saporita, C. Carfagna, P. Natanti, R. Seraglia, B. Milani, *Organometallics* 28 (2009) 4464.
- [42] A. Klein, A. Dogan, M. Feth, H. Bertagnolli, *Inorg. Chim. Acta* 343 (2003) 189.
- [43] D.J. Tempel, L.K. Johnson, R.L. Huff, P.S. White, M. Brookhart, *J. Am. Chem. Soc.* 122 (2000) 6686.
- [44] A. Zucca, M.A. Cinellu, M.V. Pinna, S. Stoccoro, G. Minghetti, M. Manassero, M. Sansoni, *Organometallics* 19 (2000) 4295.
- [45] S. Stoccoro, B. Soro, G. Minghetti, A. Zucca, M.A. Cinellu, *J. Organomet. Chem.* 679 (2003) 1.
- [46] V. Khlebnikov, A. Meduri, H. Mueller-Bunz, T. Montini, P. Fornasiero, E. Zangrando, B. Milani, M. Albrecht, *Organometallics* 31 (2012) 976.
- [47] B. Milani, A. Anzilutti, L. Vicentini, A. Sessanta o Santi, E. Zangrando, S. Geremia, G. Mestroni, *Organometallics* 16 (1997) 5064.
- [48] W. Kabsch, *Acta Cryst. D* 66 (2010) 125.
- [49] M.C. Burla, R. Caliendo, M. Camalli, B. Carrozzini, G.L. Cascarano, C. Giacovazzo, A. Mallamo, A. Mazzzone, G. Polidori, R. Spagna, *J. Appl. Cryst.* 45 (2012) 357.
- [50] G.M. Sheldrick, *Acta Cryst. A* 64 (2008) 112.
- [51] P. Emslev, K. Cowtan, *Acta Cryst. D* 60 (2004) 2126.